Int. J. Electrochem. Sci., 12 **(2017)** 11455 – 11464, doi: 10.20964/2017.12.18

International Journal of ELECTROCHEMICAL SCIENCE
www.electrochemsci.org

Influence of Surface Oxidation of Nickel-Coated Carbon Fibre on Oxygen Evolution Reaction in Alkaline Solution

Tomasz Mikolajczyk[*], *Boguslaw Pierozynski*

Department of Chemistry, Faculty of Environmental Management and Agriculture, University of Warmia and Mazury in Olsztyn, Plac Lodzki 4, 10-727 Olsztyn, Poland
[*]E-mail: tomasz.mikolajczyk@uwm.edu.pl

Received: 12 September 2017 / *Accepted:* 21 October 2017 / *Published:* 12 November 2017

This work reports on oxygen evolution reaction (OER), studied at nickel-coated carbon fibre (NiCCF) electrodes. The OER was examined comparatively on non-oxidized and electrooxidized NiCCF 12K50 tow materials in 0.1 M NaOH solution for the potential range: 1600-1800 mV vs. RHE. Electrochemical modification of NiCCF electrode results in significant facilitation of the OER kinetics, manifested through reduced, ac. impedance-derived values of charge-transfer resistance parameter and considerably modified Tafel polarization slopes.

Keywords: NiCCF; OER; Electrochemical impedance spectroscopy; NiOOH.

1. INTRODUCTION

Hydrogen economy has become an important aspect of the development of renewable energy sources, primarily due to superior properties of hydrogen as an energy carrier (its high energy-density, combined with environmental friendliness). One of the best ways to produce ultra-pure hydrogen is to carry-out the process of alkaline water electrolysis (AWE) powered by renewable energy sources, e.g. solar or wind power [1, 2]. A large number of studies can be found in literature regarding the development of novel functional catalysts designed for cathodic part of this process [3-5]. However, water splitting is mostly inhibited by its anodic part (oxygen evolution reaction: OER), which consumes a significant amount of energy [6]. Therefore, numerous recently published academic works have been devoted to developing highly-catalytic materials for the OER, in relation to alkaline water electrolysis. These research articles concentrate on the examination of metal oxides, including platinum group metals (Ru, Ir) [7, 8], as well as base metals (e.g. Ni, Mn, Fe and Co) [9-10]. Although metal oxides have superior catalytic properties towards the OER, they possess major disadvantage, which is their relatively poor electrical conductivity. A suitable solution to this problem could be in

utilization of carbon fibres as a base material for electrodes fabrication, because of their high surface area, conductivity, and excellent corrosion resistance.

Present work focuses on the impedance (kinetic) study of the OER, which is performed on non-oxidized and oxidized Toho-Tenax nickel-coated carbon fibre (NiCCF) 12K50 tow (12,000 single filaments of ca. 7.5 mm diameter and about 45 wt.% Ni) electrodes in contact with 0.1 M NaOH supporting electrolyte.

2. EXPERIMENTAL

In this work, all solutions were prepared from ultrapure water delivered by a Millipore ultrapure water purification system (Millipore Direct-Q3 UV) with 18.2 MΩ cm final water resistivity. Alkaline, 0.1 M NaOH solution was prepared from AESAR, 99.996% NaOH pellets (semiconductor grade). Before conducting experiments, atmospheric air was removed from the solution by bubbling with high-purity argon (Ar 6.0 grade, Linde).

An electrochemical cell used in this study contained a NiCCF-based working electrode (WE) in a central part, a reversible Pd hydrogen electrode (RHE) as a reference and a Pt counter electrode (CE), both placed in separate compartments. In this work, "as received" Toho-Tenax 12K 50 NiCCF tow electrodes (m_s= 43.5 mg, S_A= 84.9 cm^2) were initially de-sized in acetone, in order to remove a protective epoxy resin coating. Electrooxidation conducted on nickel-coated carbon fibre samples was performed by cycling voltammetry treatment (see Fig. 1 and its caption for details).

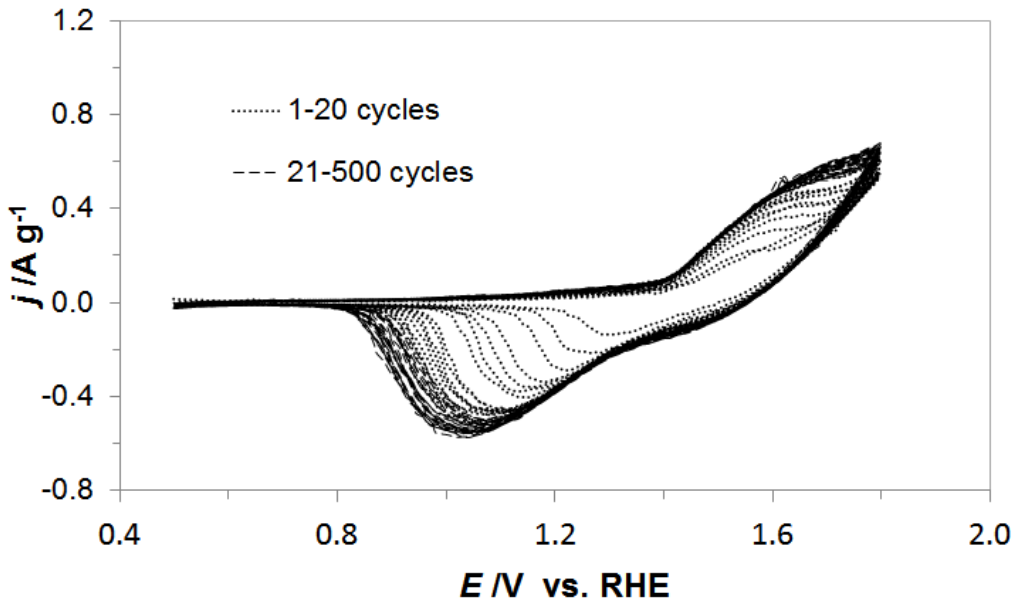

Figure 1. Cyclic voltammogram for development of nickel oxy-hydroxide layer on Toho-Tenax 12K 50 NiCCF electrode (500 CV sweeps between 0.5 and 1.8 V/RHE, carried-out at a sweep rate of 200 mV s^{-1}).

Electrochemical experiments conducted in this study included: a.c. impedance, cyclic voltammetry and quasi steady-state polarization techniques, carried-out by means of *Solartron* 12,608 W Full Electrochemical System (1260 frequency response analyser and 1287 electrochemical interface units). All supplementary information regarding the preparation of electrolytes, electrochemical cell, counter and reference electrodes, as well as specific pre-treatments employed to working electrodes and protocols for electrochemical measurements, have recently been discussed in other works from our laboratory [11, 12].

Besides, a Quanta FEG 250 scanning electron microscope (SEM) unit was employed for spectroscopic characterization of the NiCCF tow electrodes. Furthermore, a spectrophotometry (WTW, Photoflex Turb) analysis was used to account for nickel loss through the experiments.

3. RESULTS AND DISCUSSION

3.1. SEM characterization of NiCCF 12K50 tow electrodes

A comparison of two SEM micrograph pictures taken for the non-oxidized (NiCCF nox.) and oxidized (NiCCF ox.) nickel-coated carbon fibre samples is shown in Figs. 2a and 2b, respectively.

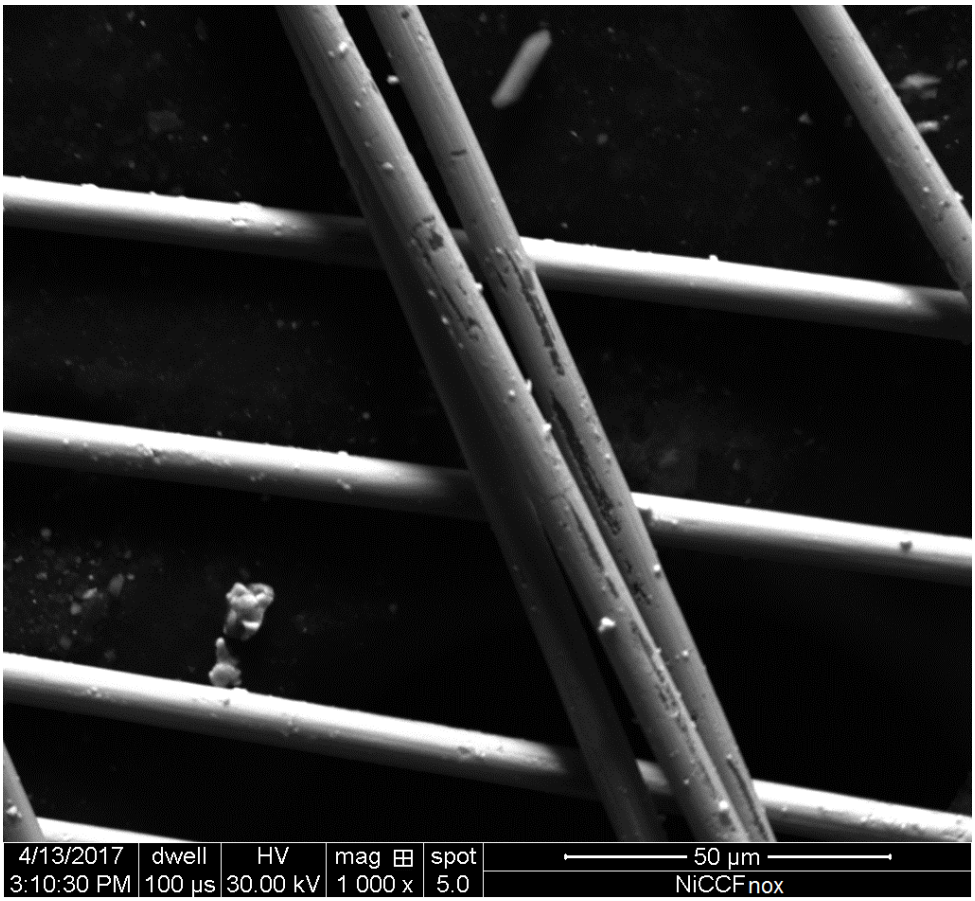

A

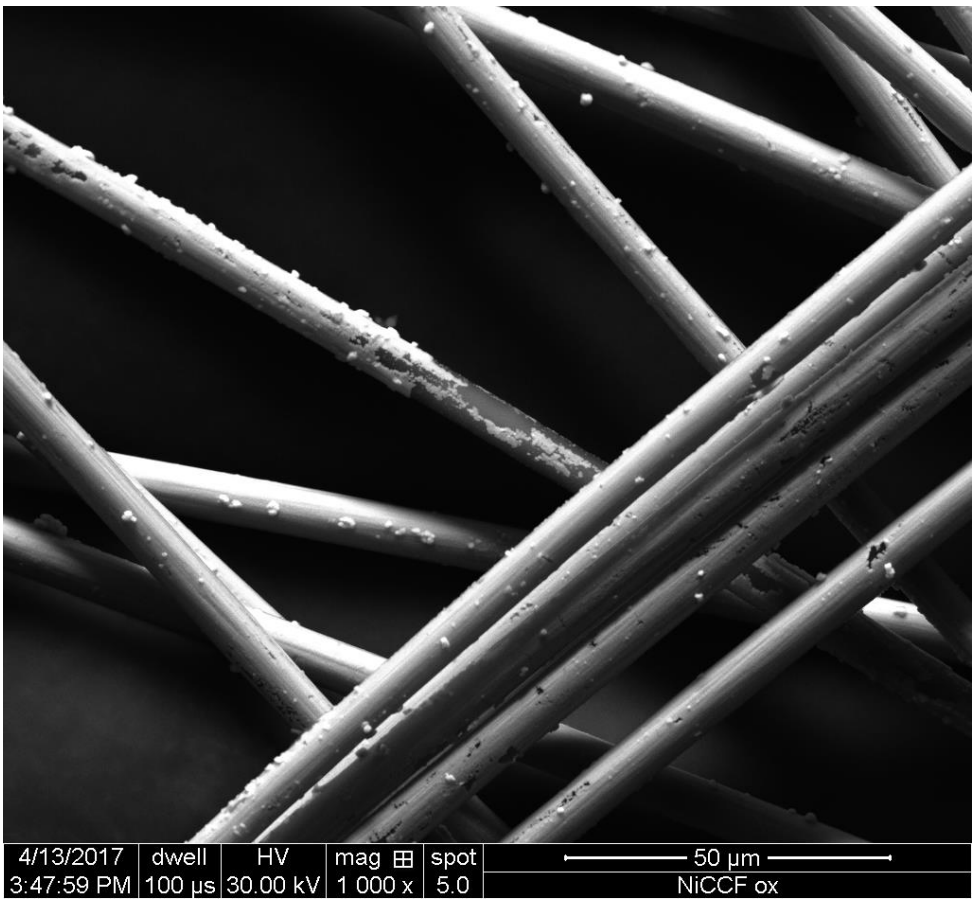

B

Figure 2. a) SEM micrograph picture of non-oxidized Toho-Tenax 12K50 NiCCF tow electrode, taken at 1,000× magnification; b) As in (a), but for oxidized NiCCF electrode.

Although it might be deduced that extended electrochemical oxidation treatment could lead to partial damage of nickel coating, the overall nickel loss is rather insignificant and it does not have any impact on the electrochemical activity of such-prepared catalyst materials (registered Ni^{2+} ion concentration in the solution after oxidation of the NiCCF electrodes would come to below 0.1 % of total Ni weight within the NiCCF tow material).

3.2. Oxygen evolution reaction on non-oxidized and oxidized NiCCF tow electrodes in 0.1 M NaOH

A.c. impedance characterization of the OER on the non-oxidized (NiCCF nox.) and the oxidized NiCCF (NiCCF ox.) tow electrodes in 0.1 M NaOH is shown in Fig. 3 and Table 1. Both examined electrodes exhibited two "depressed", partial semicircles, clearly visible in the impedance plots at all examined electrode potentials (see the recorded Nyquist impedance plots in Fig. 3). The OER impedance parameters for both electrodes were derived based on the equivalent circuit model (Fig. 4), which contained two CPE-*R* elements, where the high-frequency semicircle corresponds to the process of electron transfer for the oxygen evolution reaction, whereas the low-frequency arc is related to the kinetics of the adsorption of reaction intermediates on the electrode surface [10, 13-15].

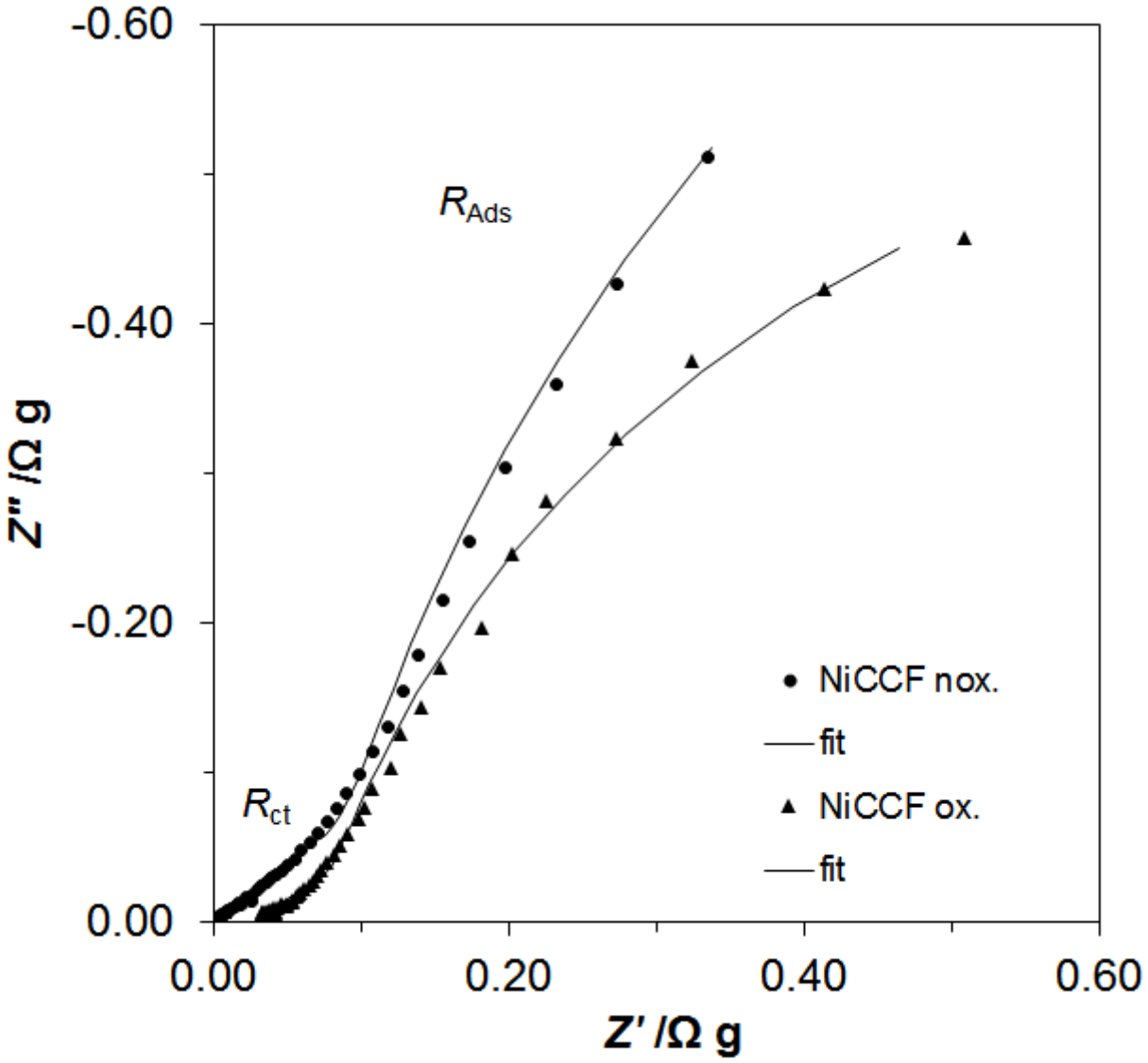

Figure 3. Complex-plane Nyquist impedance plots for the OER, recorded on non-oxidized and oxidized Toho-Tenax 12K50 NiCCF tow electrodes in contact with 0.1 M NaOH solution (carried-out at room temperature for the potential of 1500 mV vs. RHE). The solid lines correspond to a representation of the data according to the equivalent circuit shown in Figure 4, whereas points are experimental results.

Table 1. Electrochemical parameters for the OER, obtained on the non-oxidized NiCCF and electrochemically oxidized NiCCF electrodes in contact with 0.1 M NaOH. The results were derived by fitting the two CPE-*R* element (Fig. 4) equivalent circuit to the experimentally obtained impedance data (reproducibility typically below 15 %, $\chi^2 = 4\times10^{-5}$ to 2×10^{-3}).

***E*/mV**	**R_{ct}/Ω g**	**C_{dl}/μF $g^{-1}s^{\varphi 1-1}$**	**R_{ads}/Ω g**	**C_{ads}/μF $g^{-1}s^{\varphi 2-1}$**
NiCCF nox.				
1500	0.167 ± 0.030	747,011 ± 116,235	6.525 ± 0.333	969,195 ± 155,071

1525	0.112 ± 0.010	747,862 ± 30,288	1.285 ± 0.039	1,633,333 ± 108,780
1550	0.054 ± 0.005	530,437 ± 24,400	0.335 ± 0.012	1,133,333 ± 49,413
1575	0.033 ± 0.003	108,471 ± 13,570	0.159 ± 0.005	1,201,793 ± 65,257
1600	0.027 ± 0.001	73,639 ± 3,343	0.084 ± 0.002	1,410,322 ± 47,246
NiCCF ox.				
1500	0.067 ± 0.006	919,540 ± 50,851	3.785 ± 0.059	1,957,086 ± 17,483
1525	0.040 ± 0.003	881,494 ± 43,898	1.915 ± 0.231	1,980,966 ± 65,768
1550	0.034 ± 0.002	750,782 ± 33,260	0.341 ± 0.038	2,009,770 ± 56,274
1575	0.027 ± 0.003	524,552 ± 49,570	0.138 ± 0.000	2,239,195 ± 150,026
1600	0.024 ± 0.001	424,000 ± 11,618	0.062 ± 0.002	2,450,345 ± 78,656

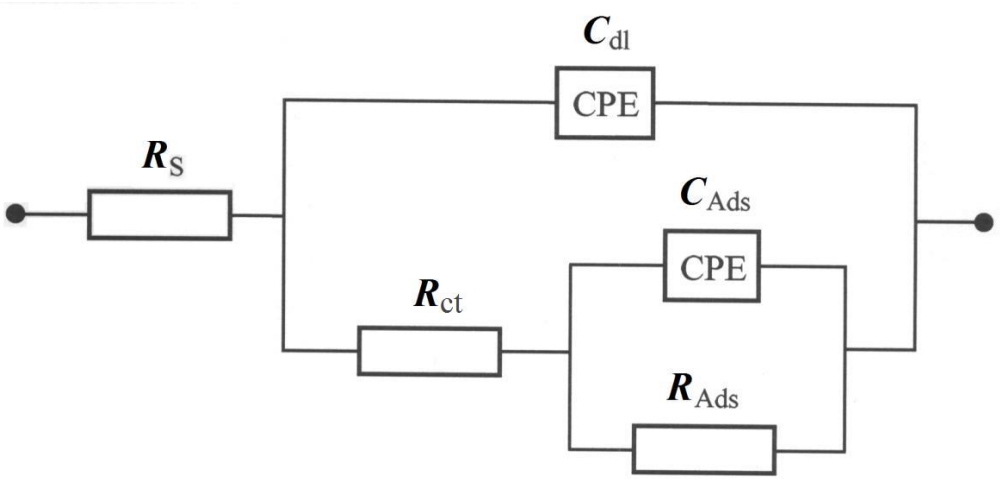

Figure 4. 2 CPE-*R* equivalent circuit used for fitting the impedance data for non-oxidized and electrooxidized Toho-Tenax 12K50 NiCCF tow electrodes. R_{ct} and C_{dl} (as CPE) elements correspond to the OER charge-transfer resistance and double-layer capacitance components, respectively; R_{Ads} and C_{Ads} (as CPE) parameters refer to the resistance imposed by the surface-adsorbed reaction intermediates and pseudocapacitance; R_{sol} is solution resistance.

Therefore, for the NiCCF nox. electrodes the recorded R_{ct} parameter decreased from 0.167 Ω g at the potential of 1500 mV (η= 270 mV) to 0.027 Ω g for the potential of 1600 mV vs. RHE (η= 370 mV). At the same time, the C_{dl} decreased from 747,011 to 73,639 μF $g^{-1}s^{\varphi 1-1}$ for the same potential range. Similarly, the R_{ct} parameter values obtained for the NiCCF ox. electrodes diminished from

0.067 Ω g to 0.024 Ω g for the same electrode potentials. Furthermore, the recorded values of the C_{dl} parameter at the potential range: 1500 to 1600 mV came to 919,540 and 424,000 μF $g^{-1}s^{\varphi 1-1}$, correspondingly. The latter effect (for both examined cases) most likely results from partial blocking of electrochemically active electrode surface by freshly formed O_2 bubbles, something that one could clearly visualise for a complex NiCCF electrode structure, especially at increased overpotentials.

The above means a significant reduction of the R_{ct} parameter for the oxidized NiCCF electrode, as compared to those of the R_{ct} values recorded for the unmodified NiCCF surface (ca. 2.5× at the potential of 1500 mV), see Table 1 for details. At higher potentials, the difference between electrochemical activity of electrodes (expressed by the R_{ct} parameter) almost disappeared, probably because the system moved into the diffusion limitation control. Additionally, the R_{Ads} parameter values for low-frequency semicircle also diminished from 6.525 and 3.785 Ω g to 0.084 and 0.062 Ω g over the studied potential range: 1500-1600 mV respectively, for the non-oxidized and the oxidized nickel-coated carbon fibre electrode. Besides, the respective values of the C_{Ads} were quite stable over the studied potential range (Table 1). Furthermore, dimensionless φ_1 and φ_2 parameters (φ determines the constant phase angle in the complex-plane plot and $0 \leq \varphi \leq 1$) of the CPE circuits (see Fig. 4) varied between 0.50-0.77 and 0.67-0.95, respectively for both examined electrodes.

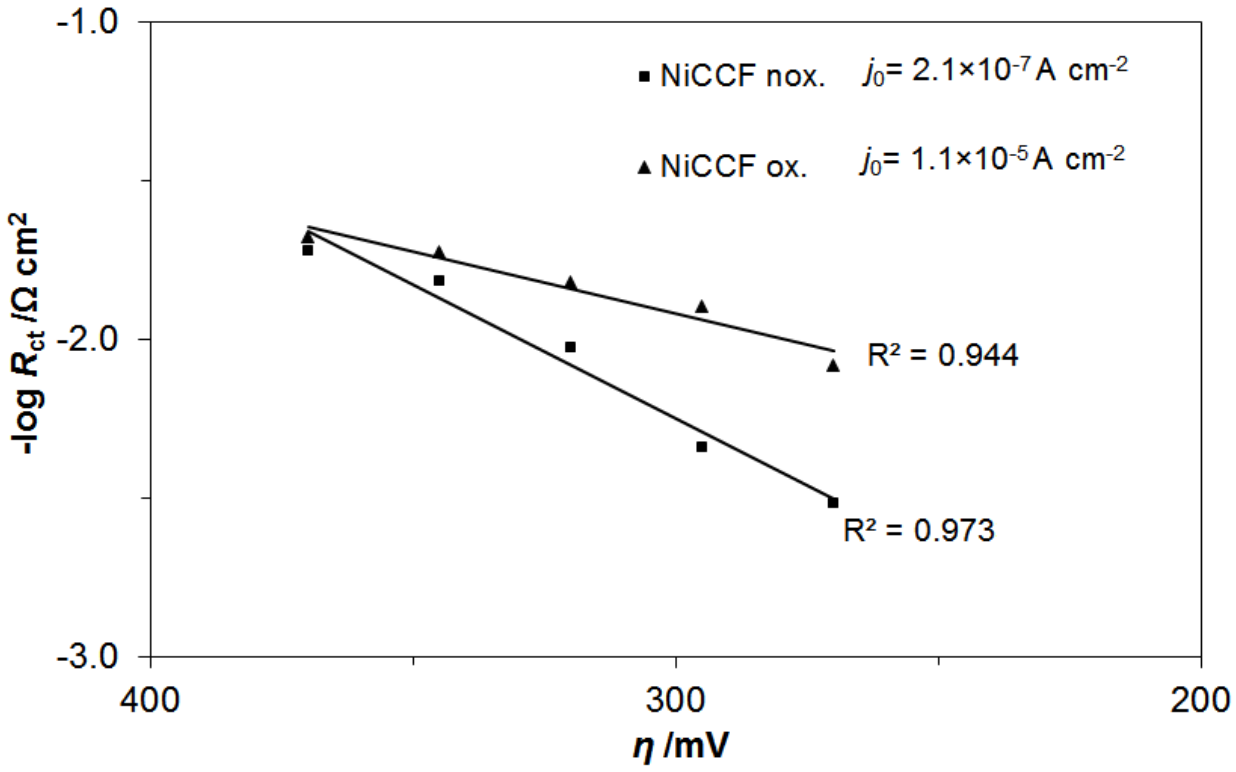

Figure 5. –log R_{ct} vs. overpotential relationship, obtained for non-oxidized and oxidized Toho-Tenax 12K50 NiCCF tow electrodes.

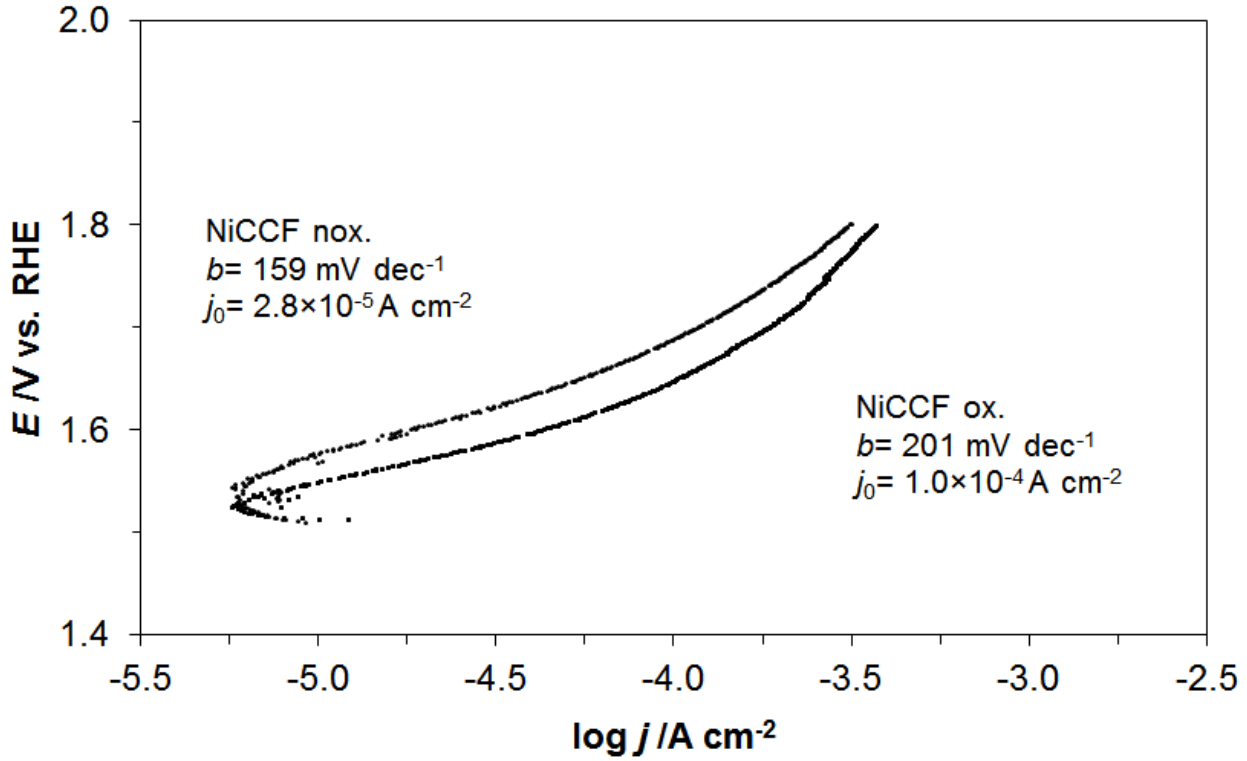

Figure 6. Quasi-potentiostatic anodic Tafel polarization curves (recorded at a rate of 0.5 mV s^{-1}) for non-oxidized and oxidized Toho-Tenax 12K50 NiCCF tow electrodes in contact with 0.1 M NaOH solution.

Based on the linear relationship: –log R_{ct} vs. overpotential (η) exhibited here over the studied overpotential range: 270-370 mV (Fig. 5), the exchange current-densities for the OER were derived based on the Butler-Volmer equation and through utilization of the relation between the exchange current-density (j_0) and the R_{ct} parameter for overpotential approaching zero [15-18]. Hence, the calculated values of the j_0 parameter for low η range came to 2.1×10^{-7} and 1.1×10^{-5} A cm^{-2} for the unmodified and the electrooxidized NiCCF materials, correspondingly. The j_0 parameter for high η could not be estimated from the impedance spectroscopy measurements, because the Nyquist plots became ambiguous for the high overpotential range. The latter is probably caused by increased rate of formation/desorption of oxygen bubbles from the electrode surface. On the other hand, the exchange current-density parameter for high η range was solely derived from Tafel plots. The recorded j_0 values came to 2.8×10^{-5} and 1.0×10^{-4} A cm^{-2} for the non-oxidized and the oxidized NiCCF, with anodic Tafel b slope ranging from 159 to 201 mV dec^{-1}, respectively.

Hence, the obtained exchange current-densities presented in this publication came out to be significantly greater than those of other OER works [16, 18-21]. For example, the j_0 parameter values recorded for various porous nickel-based electrode structures (examined in analogous alkaline solutions) ranged from 4.4×10^{-11} to 8.8×10^{-8} A cm^{-2} for low η and about 7.3×10^{-6} A cm^{-2} for high η range. The received considerably higher values of the j_0 parameter for investigated NiCCF-based electrodes are probably caused by variations in the derivation of electrochemically active surface area (the geometrical surface area was used in this work, whereas C_{dl}-based surface area estimations were employed in Refs. 16, 18 and 20).

Then, taking into account the characteristics of the oxygen evolution anodic oxidation process, one should expect that the OER kinetics on initially unoxidized NiCCF electrode should improve in time of its NaOH exposure under oxidative conditions. Yet, there was no such evidence in consecutively obtained electrochemical parameters to prove that. The above could be explained by the series of publications from the laboratory of Jerkewicz on the formation of nickel oxy- hydroxides [22-24]. Hence, in order to produce a stable and thick layer of β-NiOOH, it is necessary to follow a specified surface oxidation protocol. Otherwise, the produced oxide layer will not exhibit its full OER catalytic potential, or else such electrode could suffer from significant ageing, thus inducing quick deterioration of the OER's kinetics [25].

4. CONCLUSIONS

Nickel-coated carbon fibre material is relatively inexpensive and exhibits highly-catalytic properties towards oxygen evolution in alkaline media. Employment of specific surface electrooxidation treatment caused radical enhancement of the OER catalytic properties for NiCCF tow electrode, without cosiderable increase of its electrochemically active surface area. In conclusion, obtained results imply substantial opportunities for the application of electrooxidized nickel-coated carbon fibre 12K tow materials in industrial alkaline water electrolysers.

References

1. Y. Cheng and S. P. Jing, *Prog. Nat. Sci-Mater.*, 25 (2015) 545.
2. P. Esmaili, I. Dincer and G.F. Naterer, *Int. J. Hydrogen Energy*, 37 (2012) 7365.
3. R. Solmaz, A. Gundogdu, A. Doner and G. Kardas, *Int. J. Hydrogen Energy*, 37 (2012) 8917.
4. E. Verlato, S. Cattarin, N. Comisso, A. Gambirasi, M. Musiani and L. Vazquez-Gomez, *Electrocatalysis*, 3 (2012) 48.
5. X. Zhang, D. Wu and D. Cheng, *Electrochim. Acta*, 246 (2017) 572.
6. T. Zhou, Z. Cao, P. Zhang, H. Ma, Z. Gao, H. Wang, Y. Lu, J. He, and Y. Zhao, *Sci. Rep*., 7 (2017) 46154.
7. J.C. Cruz, V. Baglio, S. Siracusano, V. Antonucci, A.S. Aricò, R. Ornelas, L. Ortiz-Frade, G. Osorio-Monreal, S.M. Durón-Torres and L.G. Arriaga, *Int. J. Electrochem. Sci*., 6 (2011) 6607.
8. A. Di Blasi, C. D'Urso, V. Baglio, V. Antonucci, A.S. Arico', R. Ornelas, F. Matteucci, G. Orozco, D. Beltran, Y. Meas and L.G. Arriaga, *J. Appl. Electrochem*., 39 (2009) 191.
9. L. Trotochaud, J.K. Ranney, K.N. Williams and S.W. Boettcher, *J. Am. Chem. Soc*., 134 (2012) 17253.
10. R.L. Doyle and M.E.G. Lyons, *Phys. Chem. Chem. Phys*., 15 (2013) 5224.
11. B. Pierozynski and T. Mikolajczyk, *Pol. J. Chem. Technol*., 17(1) (2015) 18.
12. B. Pierozynski, T. Mikolajczyk and I.M. Kowalski, *J. Power Sources*, 271 (2014) 231.
13. F.R. Costa, D.V. Franco and L.M. Da Silva, *Electrochim. Acta*, 90 (2013) 332.
14. M.E.G. Lyons and M.P. Brandon, *Int. J. Electrochem. Sci*., 3 (2008) 1386.
15. D.V. Franco, L.M. Da Silva, W.F. Jardim and J.F.C. Boodts, *J. Braz. Chem. Soc*., 17 (2006) 746.
16. T. Kessler, W.E. Triaca and A.J. Arvia, *J. Appl. Electrochem*., 24 (1994) 310.
17. R.L. Doyle and M.E.G. Lyons, Photoelectrochemical Solar Fuel Production, (2016) Springer International Publishing, Switzerland.

18. B.M. Jović, U.Č. Lačnjevac, V.D. Jović and N.V. Krstajić, *J. Electroanal. Chem*., 754 (2015) 100.
19. J. Kubisztal and A. Budniok, *Int. J. Hydrogen Energy*, 33 (2008) 4488.
20. B.M. Jović, V.D. Jović, U.Č. Lačnjevac, Lj. Gajić-Krstajić and N.V. Krstajić, Zastita Materijala 57 (2016) 136.
21. C. Bocca, A. Barbucci and G. Cerisola, *Int. J. Hydrogen Energy*, 23 (1998) 247.
22. M. Alsabet, M. Grden and G. Jerkiewicz, *Electrocatalysis*, 2 (2011) 317.
23. M. Alsabet, M. Grden and G. Jerkiewicz, *Electrocatalysis*, 5 (2014) 136.
24. M. Alsabet, M. Grden and G. Jerkiewicz, *Electrocatalysis*, 6 (2015) 60.
25. S.R. Mellsop, A. Gardiner and A.T. Marshall, *Electrochim. Acta*, 180 (2015) 501.